Metallophysics and Advanced Technologies
Металофіз. новітні технол.
Metallofiz. Noveishie Tekhnol.
2023, vol. 45, No. 3, pp. 403–421
https://doi.org/10.15407/mfint.45.01.403
Reprints available directly from the publisher

PACS numbers: 46.55.+d, 62.20.Qp, 62.40.+i, 81.40.Lm, 81.40.Pq

The Influence of Structuring Surfaces and Slide Burnishing on Tribological Properties

W. Koszela, P. Bałon[*,**], S. E. Rejman[***], B. Kiełbasa[*], R. Smusz[***], and M. Bembenek[**]

Rzeszow University of Technology,
Department of Manufacturing Processes and Production Engineering,
al. Powstańcyw Warszawy 12,
PL-35959 Rzeszow, Poland
[*]*ZPU Mirosław Pogoda,*
al. Wojska Polskiego 36,
PL-39300 Mielec, Poland
[**]*AGH University of Science and Technology,*
Faculty of Mechanical Engineering and Robotics,
al. Mickiewicza 30-B2,
PL-30059 Krakow, Poland
[***]*Rzeszow University of Technology, Department of Machine Design,*
al. Powstańcyw Warszawy 12,
PL-35959 Rzeszow, Poland

The shaping of sliding surfaces of steel parts and friction pairs is a great potential for solving problems in the field of sliding pairs, such as: reduction of friction resistance, increase in lift, control of slotted flows, heat dissipation, and increasing the durability of friction pairs. The article presents tribological tests of a mapped sliding node based on selected vane pump components. The tests are carried out on the T-11 tribological tester (pin on disc) and are comparative in relation to standard elements. Surface changes in the tested friction nodes include the use of two additional machining processes, *i.e.*, slide burnishing and texturing. The material for the samples is carbonitrided and heat-treated C22E steel, while the material for the counter-samples is E295 steel with a hardness of 160 *HB* (non-heat-treated). The use of addi-

Corresponding author: Michał Bembenek
E-mail: bembenek@agh.edu.pl

Citation: W. Koszela, P. Bałon, S. E. Rejman, B. Kiełbasa, R. Smusz, and M. Bembenek, The Influence of Structuring Surfaces and Slide Burnishing on Tribological Properties, *Metallofiz. Noveishie Tekhnol.*, **45**, No. 3: 403–421 (2023).
DOI: 10.15407/mfint.45.03.0403

tional processes in the form of burnishing and texturing on the sliding surfaces significantly reduces the friction coefficient by about 15% and reduces the resistance to movement for the tested combination. Tribological tests are carried out in two variants, *i.e.*, with a constant sliding speed and variable load as well as with constant load and variable sliding speed about 50%. The authors conduct a number of studies, the results of which can be found in this work, in particular, for applications for the co-operation of parts of injection pumps.

Key words: steel, surface structuring, slide burnishing, texturing, lubrication pockets, tribological properties.

Вивчення процесів формування поверхонь ковзання крицевих деталів і пар тертя уможливлює вирішення цілого ряду проблем, пов'язаних із парами ковзання, таких як: зменшення опору тертя, збільшення підйомної сили, керування щілинними потоками, розсіяння тепла та підвищення довговічности пар тертя. У статті представлено результати трибологічних випробувань, які моделюють вузол ковзання на основі обраних компонентів лопатевого насоса. Випробування проводилися на триботестері T-11 (схема тертя штифта по диску) та порівнювалися зі схемами із стандартних елементів. Зміни поверхні в тестованих вузлах тертя включали використання двох додаткових процесів механічного оброблення, а саме, вигладжування ковзанням і текстурування. Матеріялом для зразків було азотовано та термічно оброблено крицю C22E, а матеріялом для контрзразків було обрано крицю E295 із твердістю у 160 *HB* (без термообробленя). Застосування додаткового оброблення у вигляді вигладжування та текстурування на поверхнях ковзання значно понизило коефіцієнт тертя (приблизно на 15%) та зменшило опір руху для досліджуваної комбінації. Трибологічні випробування проводились у двох варіянтах, а саме, з постійною швидкістю ковзання та змінним навантаженням і з постійним навантаженням та змінною швидкістю ковзання близько 50%. Результати досліджень, наведені в даній роботі, можуть бути використані, зокрема для застосування під час виготовлення деталів інжекторних насосів.

Ключові слова: криця, поверхневе структурування, ковзне вигладжування, текстурування, мастильні кишені, трибологічні властивості.

(Received February 13, 2023; in final version, February 28, 2023)

1. INTRODUCTION

Changes occurring in the elements of injection pumps, especially the supply pumps caused by friction forces and physical and chemical phenomena occurring during the operation of a diesel engine pump, are called scuffing. As a result of attraction, there is a continuous change in dimensions, loss of material or plastic deformation of some parts working in the supply pump (vane) or the injection pump of a diesel engine. Theoretical analysis of cyclic sliding in frictional contact [1], behaviour of coated parts under local load [2–5], contact interaction in damaged

TABLE 1. The chemical composition of C22E steel.

Mn	Si	P	S	Cr	Ni	Mo	Cu	Al
0.17–0.24	0.35–0.65	0.15–0.40	< 0.040	< 0.040	< 0.3	< 0.3	< 0.1	< 0.1

bodies [6] are often useful for explaining wear phenomena. The papers [7–9] present the methods to determine contact stresses on the surfaces of conjugate parts and to specify a relation between the maximum operational loads and slip zone dimensions for friction contact. There are many methods to reduce or eliminate the phenomenon of wear [10]. The most commonly used include heat treatment (surface hardening), thermochemical treatment (hardening nitriding, carburizing), plastic processing (burnishing, structuring), and coatings.

The authors [11, 12] proposed the concept of a rational choice of materials for the manufacture of parts; and the papers [13–15] developed theoretical approaches to select the composition of materials and technological parameters for the strengthening process. Optimizations of manufacturing processes are used to increase machine part durability [16], including taking into account technological heredity [17, 18] to ensure the reliable functioning of products with coatings during the life cycle [19]. High-quality balancing [20] and stable lubrication of moving elements of friction pairs [21] are necessary to ensure reliable operation of machines and mechanisms.

The structuring of rubbing surfaces has a significant impact on the processes occurring in the sliding association. The surface condition is the dominant quality factor in a tribological node [22]. Increasing the durability and efficiency of machines and devices, among others attributes, by limiting unfavourable friction phenomena, prompts the

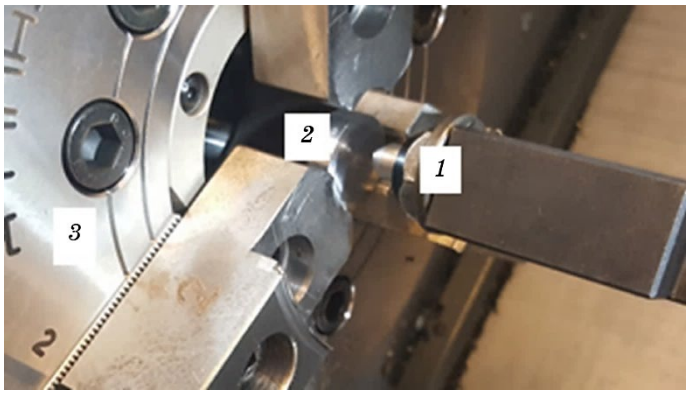

Fig. 1. The process of sliding burnishing of the sample surface: *1*—DB-3 burnishing tool, *2*—sample, *3*—three-jaw chuck.

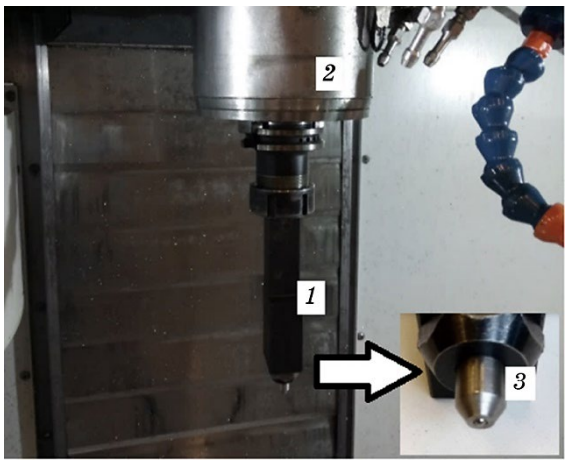

Fig. 2. DB-3 burnishing tool adapted for structuring counter-samples: *1*—DB-3 burnishing tool, *2*—CNC milling spindle, *3*—forming element.

search for surface treatment technologies that will positively affect the reduction of resistance to movement and wear [23].

To protect pump parts from wear and corrosion, coatings applied in various ways are used, for example, electrochemical chromium plating in a calm electrolyte [24, 25] and flowing electrolyte [26–28], diamond-galvanic coatings [29] electrospark alloying [30–32], laser alloying [33], ion-plasma coatings [34], plasma electrolytic oxidation [35–37] and surfacing [38–41] *etc*.

Various technological methods are also used to improve the operational properties of machine parts. Among them stand out: surface plastic deformation—ultrasonic impact treatment [42, 43] and vibration treatment with steel balls [44], friction strengthening treatment

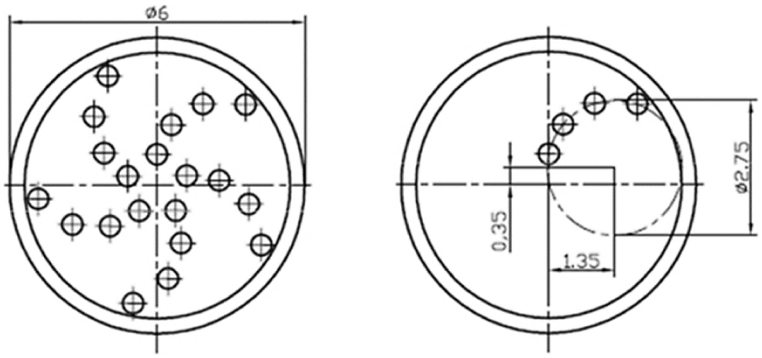

Fig. 3. Distribution of depressions on the surface of the counter-sample (fragment of the working drawing).

TABLE 2. Technical data of the tribological test stand (T-11).

Technical data	
Movement type	Sliding
Contact geometry	Diffused or concentrated
Nominal diameter of the disc	25.4 mm (1″)
Sliding speed	to 0.6 m/s
Load	to 50 N
Friction radius	to 10 mm
Temperature in the test chamber	to 300°C

[45–47], diamond polishing of steels and coatings [48–50]. Such processing allows you to smooth out irregularities, reduce roughness, and create the necessary microprofile of the part surfaces. In addition, residual compressive stresses are formed in the surface layer and its hardness increases, which provides a corresponding increase in fatigue strength under cyclic loads and wear resistance of parts, as well as corrosion resistance.

The choice of the basic technology for shaping a specific geometric surface (SGP) is hampered by the variety of machine elements mainly due to their shape, dimensions, surface roughness, heat treatment, accuracy of workmanship, material used, coatings, *etc.* [51]. For this reason, there is a need to adapt already existing processing methods for texturing, modify them or designing new processing methods [52–57]. Advantage of machining units is the possibility of utilizing the advantageous features of SGP immediately after the basic machining (*e.g.*, turning or burnishing) in the same mounting. In some cases, this is essential and definitely improves the quality of texturing. In the literature or reported inventions [58–60], one can find various designs of tools cooperating with conventional or computer numerical control (CNC) machine tools.

In general, to shape specific machining marks and lubrication pockets on sliding surfaces, the technologies of ablation and non-aberration machining and (but to a lesser extent) incremental methods are used. Publication [61–63] presents exemplary methods of loss-free and lossless methods technology of shaping regular SGP.

Removal methods: machining (turning, milling, planning, drilling, *etc.*), abrasive processing (grinding, honing, oscillating superfinishing, micro-polishing, abrasive blasting, *etc.*), erosion and chemical machining (chemical and electro-chemical etching, electrical discharge machining), high-energy machining (laser treatment, electron beam treatment, high-pressure water jet treatment, plasma treatment).

Non-loss machining methods: embossing using a forming element,

sliding, oscillating, impulse, eccentric burnishing, *etc.*, sintering of metal powders with texturizing of the sliding surface.

The desired tribological features of the geometric structure of the surface are closely related to its shape and geometric parameters kinematic parts mating. They usually depend on the shaping method and way. For the surface with a shaped texture of tenths of a millimetre or larger and relatively low hardness, conventional or CNC machine tools are usually sufficient. The use of conventional machining methods to shape lubricant pockets is limited by the speed and efficiency of machining, especially for serial or mass production. With small quantities of manufactured products or samples for laboratory testing, this is acceptable. The production of items possessing more textured surfaces requires the use of tooling to improve performance or more efficient texturing methods must be used. Machine tools can also be equipped with specially designed heads or instrumentation increasing machining capabilities. This method is most often used when introducing new products with a modified sliding surface to production. The analysis of literary sources and patents showed the lack of information on the rational selection of modes of diamond smoothing of operational surfaces to form a regular relief and, accordingly, high operational characteristics of steel parts.

The aim of the conducted research was to determine the impact and usefulness of the technology of structuring friction surfaces and sliding burnishing on the tribological properties of selected elements of a vane pump. In addition, the main goal was to search for a method of significantly reducing the wear of heavily loaded cooperating elements of the pump unit and to increase their durability, including cyclical variables. The tests were comparative in relation to the reference samples, which were made in accordance with the technology used by the manufacturer of the vane pump (ZPU Mirosław Pogoda) [64, 65].

TABLE 3. Parameters of tribological tests in the load variant.

Test parameters (load variant)	
Test temperature	23–24°C
Rotation speed	150 rpm (constant)
Lubricant used	Kalibrol LUX
Amount of lubricant	4 ± 0.1 ml
Test length	1500 s
Normal load	From 10 N to 50 N in steps of 10 N
Duration of a single step	300 s

TABLE 4. Test parameters in the speed variant.

Test parameters (load variant)	
Test temperature	23–24°C
Rotation speed	From 150 to 400 rpm with a step 50 rpm
Lubricant used	Kalibrol LUX
Amount of lubricant	4 ± 0,1 ml
Test length	1800 s.
Normal load	20 N (constant)
Duration of a single step	300 s

2. EXPERIMENTAL DETAILS

2.1. The Research Program

The research program included: preparation of test samples and counter-samples, specific geometric surface measurements of reference samples and counter-samples, burnishing of samples, structuring counter-samples, specific geometric surface measurements of burnished samples, specific geometric surface measurements of textured counter-samples, tribological tests of reference samples and counter-samples, specific geometric surface measurements after tribological tests, tribological tests of samples and counter-samples after burnishing and structuring, specific geometric surface measurements after tribological tests.

2.2. The Samples

C22E type carbon steel used for the tests was used for injection pump components with good weldability, not requiring high strength properties in the heat-treated state.

In the softening annealed state, the steel is characterized by good machinability, in turn, in the normalized state, the material shows much better susceptibility to mechanical cutting (Table. 1). Importantly, the steel does not show spring-back after thermochemical treatment up to 60 *HTC*, *e.g.* after carbonitriding to a depth of 0.3–0.4 mm. For testing used simples: St. WAZ + H25 and anti-sample St. 160HB35. Statistical analysis of test results and statistical evaluation were performed with constant variance. When analysing the test results, constraints on the designated functions approximating the test results were assumed. Test results presented using regression functions for specific assumed tribological properties.

In the heat-treated state after carbonitriding, the material has the following parameters: tensile strength, $Rm = 470–650$ MPa, yield strength, $Re > 290$ MPa, elongation, $A > 20\%$, restriction, $Z > 50\%$, impact strength, $KV > 50$ J.

Particularly heavily loaded samples, subject to frictional wear, for which thermo-chemical treatment (carbonitriding) to a depth of 0.3–0.5 mm and hardening to a hardness of approx. 60 ± 2 *HRC* were used in the tests.

2.3. The Surface Treatment

In the presented article, a CNC lathe and milling machine as well as sliding burnishing equipment were used to modify the geometric structure of the surface of the samples and counter-samples. In order to carry out an additional structuring process, the burnishing element in a commercial sliding burnishing machine was modified. At this stage of the research, it was the most advantageous solution both in terms of time and in terms of cost. Sliding burnishing and structuring were carried out on a HAAS CNC lathe and milling station, using a special tool in the form of a DB-3 burnishing tool from Cogsdill [66]. Figure 1 show a sample mounted in the machine tool holder immediately after the sliding burnishing operation.

The forming element of the burnishing tool (Figure 2) was adapted to the operation of structuring the friction surfaces of the counter-samples, so that by pressing the indenter, lubricating micropockets in the shape of a spherical segment were obtained. The arrangement of the depressions on the machined surface was made in accordance with the working drawing (Fig. 3). Picks were placed on a circle with a di-

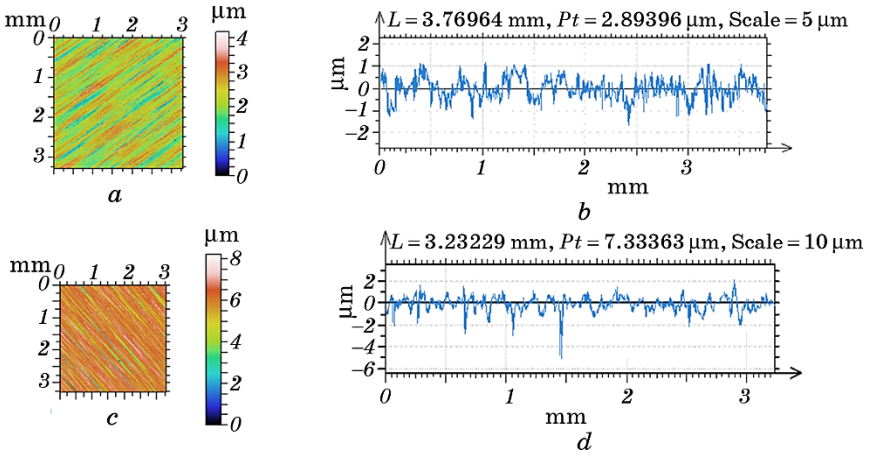

Fig. 4. Contour maps (*a*, *c*) and roughness profiles (*b*, *d*) of the St. WAZ + H1 (*a*, *b*) sample and the St. 160HB1 (*c*, *d*) counter-sample before tribological tests.

TABLE 5. Selected parameters of the surface topography of the sample St. WAZ + H1 (*a*, *b*) and the counter-sample St. 160HB1 (*c*, *d*) before tribological tests.

Surface parameter	St. WAZ + H1	St. 160HB1
S_q—mean squared deviation height of surface irregularities from the reference plane, μm	0.519	0.800
S_{sk}—skewness factor of the distribution topography heights (ordinates) surface	–0.222	–1.667
S_{ku}—distribution concentration factor topography heights (ordinates) surface	3.149	8.845
S_p—the height of the highest elevation of the 3*D* profile, μm	1.942	2.256
S_v—value of the lowest 3*D* profile recess, μm	2.229	5.980
S_z—maximum height of the 3*D* profile, μm	4.172	8.236
S_a—arithmetic mean deviation height of surface irregularities from the reference plane, μm	0.412	0.5750
S_{al}—the smallest length of the segment, at which the autocorrelation function reaches value 0.2, Mm	0.035	0.018

ameter of 2.75 mm every 0.7 mm in the arc measure, in five-fold and even distribution on the sliding surface [67–71].

2.4. The Tribological Tests

Tribological tests were carried out using the T-11 (ITEPIB) pin on disc tester. It is a tester designed to evaluate the tribological properties of friction pairs and lubricating materials operating in unidirectional slip conditions. It is used primarily for tests aimed at determining wear and resistance to motion in the tested friction node. The research association consisted of a mandrel pressed against a rotating disc with a given force. Technical data of the tribological test stand are presented in Table 2.

In order to reproduce the distributed contact, a modified counter-sample mounting system was used. In this arrangement, the counter-sample was mounted oscillatingly in order to ensure a distributed contact and to eliminate any errors in manufacturing or fixing the samples on the device. Considering the wide range of loads exerted on the mated surfaces in the real friction node, a step test was used. It consisted in cyclical increase of the load every predetermined period. Other test parameters, such as the sliding speed or the volume of the lubricant used, remained unchanged. This type of tribological tests was called the load variant and its parameters are presented in Table 3.

The second-test variant was tests with variable sliding speed. Constant load and lubricant volume were used. The rotational speed of the disc was variable, which was aimed at examining how the friction force would change as a function of variable sliding speeds. The test parameters in the speed variant are presented in Table 4.

2.5. Investigation of the Structure and Properties of the Surfaces

To perform measurements of the geometric structure of the surface (SGP), an optical device using the Talysurf CCI coherent correlation interferometry method by Taylor Hobson [72] was used, equipped with a five-fold magnification lens. A single measurement consists of a 1024 by 1024 matrix containing coordinates from surface irregularities. The measurement area was 3×3 mm. The vertical resolution was 0.01 nm. Contour maps, roughness profiles and selected surface topography parameters were used for the study. The parameters of the geometric structure of the surface were calculated and visualized using the TalyMap—Digital Surf software [73, 74].

List of abbreviations and symbols used: S_a—arithmetic average height of the surface, S_{al}—autocorrelation length, S_{pq}—mean square slope of the surface, S—coefficient of slope of the surface, S_p—height of the highest vertex of the surface, S_{pc}—average curvature of the top fillet radius, S_{pd}—vertex density, S_q—root mean square height of the surface, S_{sk}—surface asymmetry coefficient, S_{tr}—aspect ratio of the surface, St. WAZ + H—sample designation, St. 160HB—marking of the counter-sample, S_v—coefficient of the largest bottom of the sur-

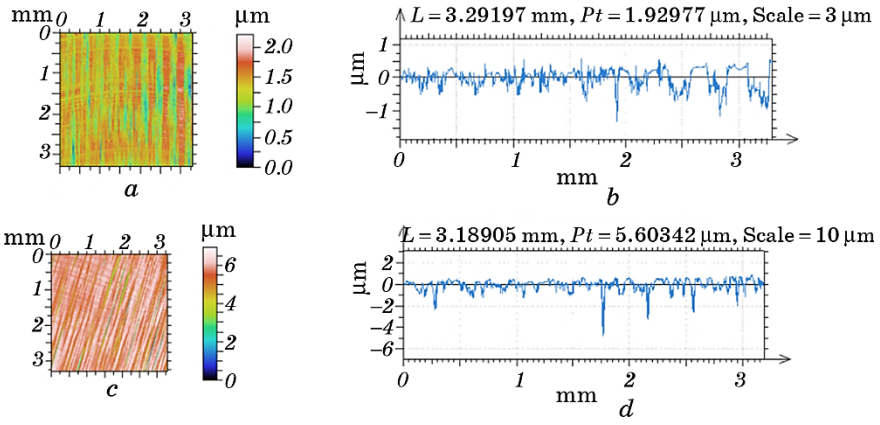

Fig. 5. Contour maps (*a*, *c*) and roughness profiles (*b*, *d*) of the St. WAZ + H1 (*a*, *b*) sample and the St. 160HB1 (*c*, *d*) counter-sample after tribological tests.

TABLE 6. Selected parameters of the surface topography of the sample St. WAZ + H1 (*a*, *b*) and the counter-sample St. 160HB1 (*c*, *d*) after tribological tests.

Surface parameter	St. WAZ + H1	St. 160HB1
S_q, μm	0.273	0.683
S_{sk}	–0.617	–2.338
S_{ku}	3.527	11.824
S_p, μm	0.879	1.258
S_v, μm	1.334	5.682
S_z, μm	2.213	6.940
S_a, μm	0.216	0.4812
S_{al}, Mm	0.0547	0.017

face, S_z—the greatest height of the surface.

3. RESULTS AND DISCUSSION

3.1. Study of Roughness

Figure 4 shows contour maps and roughness profiles, and Table 5 shows selected parameters of the surface topography of carbonitrided and hardened samples marked St. WAZ + H1 and counter-samples made of softened steel St. 160HB1 (before tribological tests). The surfaces of the sample and counter-sample were made in accordance with the technology of the manufacturer of the vane pump—ZPU Mirosław Pogoda.

The height of the surface roughness of the counter-sample was greater than the height of the roughness of the sample surface. The *Ra* parameter of the sample surface is about 0.35 μm, and the counter-sample is 0.47 μm. Both surfaces are unidirectional, anisotropic surfaces.

Figure 5 shows contour maps and roughness profiles, and Table 6 shows selected parameters of the surface topography of the St. WAZ + H1 sample and the St. 160HB1 counter-sample (after tribological tests). Traces are visible on the contour maps of the sample and counter-sample surfaces abrasion. Traces are visible on the contour maps of the sample and counter-sample surfaces abrasion. It was reduced the height of the surface roughness. The *Ra* value of the sample decreased to 0.2 μm, and the value of the antisample to 0.35 μm. The density decreased, and the radius of rounding the vertices of the mating surfaces increased.

3.2. Research Nodes with a Modified Surface

Figure 6 presents contour maps and surface unevenness profiles, and table 7 shows selected parameters of the surface topography of the St. WAZ + H25 sample and the St. 160HB35 counter-sample before tribological tests. The disc (sample) was slid burnished with a DB-3 burnisher at a constant speed of 5 m/min and a feed rate of 0.05 mm/rev., and lubrication pockets were made on the surface of the counter-sample using a CNC milling machine and a modified burnishing element.

The height of the counter-sample unevenness was greater than the height of the sample surface. However, the values of the *Ra* parameter of the sample and the counter-sample in the area free of pits were the same and amounted to about 0.35 μm. The surface of the sample is anisotropic and the counter-sample is isotropic due to the presence of dimples. The width of the pits is about 0.5 mm and the depth was about 15 μm.

Figure 7 shows contour maps and surface unevenness profiles, and

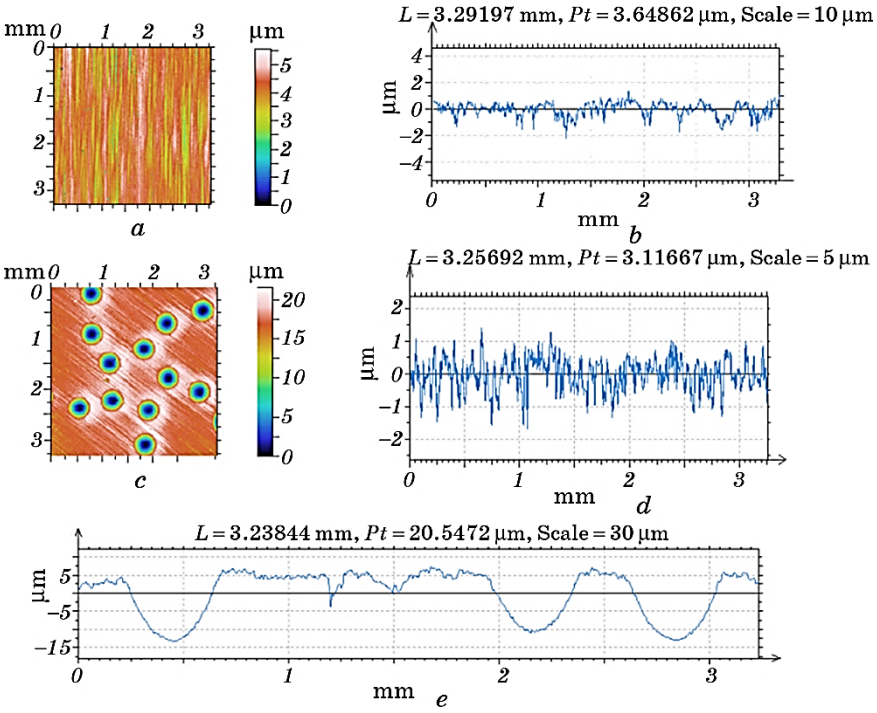

Fig. 6. Contour maps (*a*, *c*) and roughness profiles (*b*, *d*) of the St. WAZ + H25 sample (*a*, *b*) and the St. 160HB35 counter-sample (*c*, *d*) before tribological tests, Figure *e* shows the roughness profile counter-samples passing through the lubrication pockets.

TABLE 7. Selected parameters of the surface topography of the sample St. WAZ + H25 (*a*, *b*) and the counter-sample St. 160HB35 (*c*, *d*) before tribological tests.

Surface parameter	St. WAZ + H1	St. 160HB1
S_q, µm	0.529	3.921
S_{sk}	–0.934	–2.288
S_{ku}	4.608	7.767
S_p, µm	1.503	5.297
S_v, µm	4.078	16.237
S_z, µm	5.582	21.534
S_a, µm	0.409	2.491
S_{al}, Mm	0.043	0.195

Table 8 contains selected parameters of the surface topography of the St. WAZ + H25 sample and the St. 160HB35 counter-sample after tribological tests.

The heights of the sample and counter-sample unevenness decreased due to tribological wear. The dimensions of the lubrication pockets have also decreased. On the other hand, the height radii of the surface irregularities of the sample and counter-sample increased.

3.3. Tribological Tests

Tribological tests were carried out in a random order and included material pairs containing carbonitrided and hardened steel samples and steel counter-samples with a hardness of 160 HB. Two types of tests were performed: with a variable load and with a variable sliding speed. The cumulative results are shown in Figs. 8 and 9.

The coefficient of friction for the unmodified friction pair had an almost constant value regardless of the load and its average value was in the range from 0.17 to 0.175.

For tests with variable load and the use of an additional burnishing operation, the average value of the friction coefficient was reduced by 8% (worst case) and 24% (best case). A negative effect was the increase in the dispersion of results, especially at loads of 10 N and 20 N. The additional use of the structuring process resulted in the stabilization of the friction coefficient, at the expense of a slight increase in the coefficient of friction compared to burnished friction pairs.

During tests with variable rotational speed, it was shown that both modifying the mating surface by burnishing and structuring cause a significant reduction in the coefficient of friction. The best results

were obtained at higher sliding speeds.

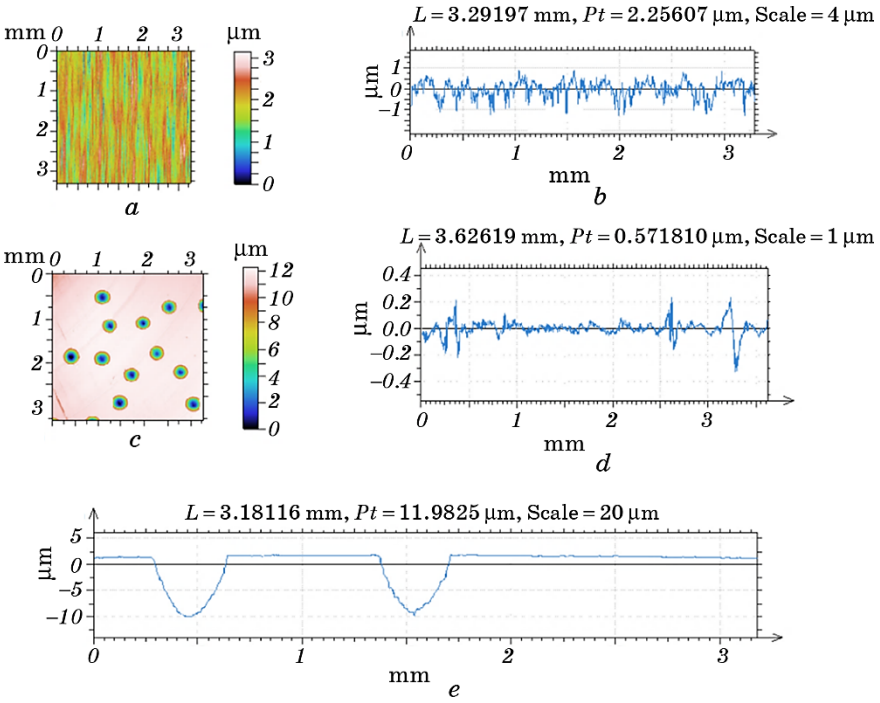

Fig. 7. Contour maps (*a*, *c*) and roughness profiles (*b*, *d*) of the St. WAZ + H25 (*a*, *b*) and counter-sample St. 160HB35 (*c*, *d*) after tribological tests, Figure *e* shows the counter-sample irregularity profile passing through the lubrication pockets.

TABLE 8. Selected parameters of the surface topography of the sample St. WAZ + H25 (*a*, *b*) and the counter-sample St. 160HB35 (*c*, *d*) after tribological tests.

Surface parameter	St. WAZ + H1	St. 160HB1
S_q, μm	0.405827	1.93428
S_{sk}	–0.57216	–3.55478
S_{ku}	3.55489	15.1913
S_p, μm	1.24705	1.20922
S_v, μm	1.88821	11.1172
S_z, μm	3.13526	12.3264
S_a, μm	0.317928	1.01653
S_{al}, Mm	0.0327806	0.172914

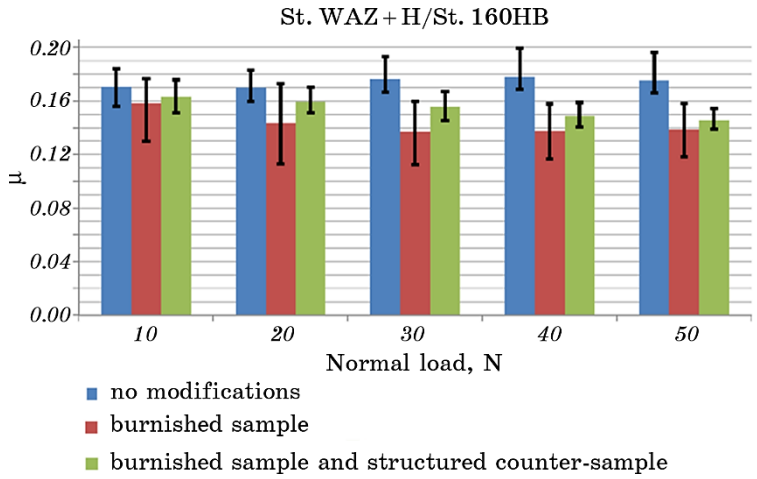

Fig. 8. Average values of the coefficient of friction depending on the normal load with the dispersion of the results.

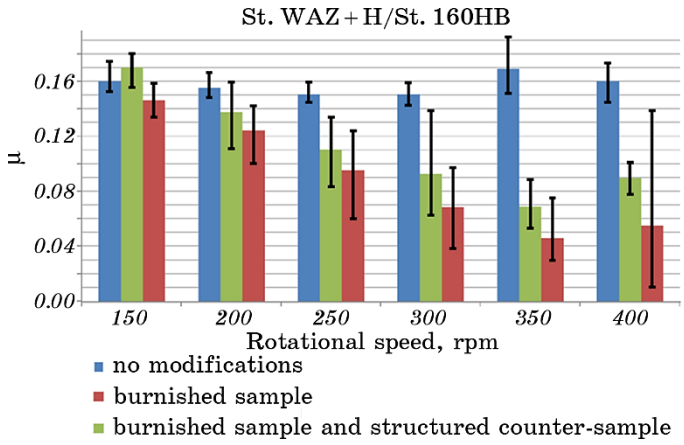

Fig. 9. Average values of the coefficient of friction depending on the rotational speed along with the dispersion of the results.

For the friction pair modified by sliding burnishing, the reduction of the friction coefficient was obtained by a maximum of 66% compared to unmodified surfaces, and in the case of burnishing and structuring by as much as 73% (for 350 rpm).

4. CONCLUSION

In the conducted tests, the relationship between the work parameters

and the parameters of the surface texture of steel parts was analysed. The texture is formed by a series of circular recesses in the shape of a sphere, the radius of which is several times greater than its depth. A very clear influence of the ratio of the microcavity depth to its diameter was found for reducing abrasion, which can be optimized for a given parameter. The analysis shows that the effectiveness of microcavities depends on hydrostatic and hydrodynamic processes inside injection pomp what has an impact on reduction of friction resistance. The use of additional processes in the form of burnishing and texturing of the sliding surfaces significantly reduced the friction coefficient by about 15% and reduced the resistance to motion for the tested joint. Because of their own research, the authors came to the following conclusions:

1. Burnishing, as a process that reduces friction and wear, achieves better results than surface structuring at low speeds, where hydrodynamic forces are probably not generated.
2. Structuring of surfaces operating at low sliding speeds leads only to the stabilization of the friction coefficient at variable loads and a reduction in the dispersion of the obtained results.
3. The hydrodynamic force generated on structured surfaces causes a very large reduction in the resistance to motion. To achieve it, it is necessary to achieve an appropriate relative sliding speed.
4. As a result of tribological tests, the height of surface irregularities decreased for both the sample and the counter-sample, and the rounding radii of the tops of the mating surfaces increased as a result of surface lapping.
5. Sliding burnishing, and especially surface structuring, can be recommended as technologies that improve cooperation in sliding nodes operating in the presence of a lubricant.

Research co-financed by the project No. RPPK.01.02.00-18-0029/19 entitled ‘R&D works on an innovative injection pump dedicated to engines of heavy vehicles and special-purpose equipment’ co-financed by the European Regional Development Fund.

REFERENCES

1. I. Yo. Popadyuk, I. P. Shats’kyi, V. M. Shopa, and A. S. Velychkovych, *J. Math. Sci.*, **215**: 243 (2016).
2. L. Y. Ropyak, I. P. Shatskyi, and M. V. Makoviichuk, *Metallofiz. Noveishie Tekhnol.*, **41**, No. 5: 647 (2019) (in Ukrainian).
3. L. Ya. Ropyak, I. P. Shatskyi, and M. V. Makoviichuk, *Metallofiz. Noveishie Tekhnol.*, **39**, No. 4: 517 (2017). (in Ukrainian).
4. M. Bembenek, M. Makoviichuk, I. Shatskyi, L. Ropyak, I. Pritula, L. Gryn, and V. Belyakovskyi, *Sensors*, **22**, No. 21: 8105 (2022).
5. I. P. Shatskyi, V. V. Perepichka, and L. Y. Ropyak, *Metallofiz. Noveishie*

Tekhnol., **42**, No. 1: 69 (2020) (in Ukrainian).
6. I. P. Shatskii, *J. Math. Sci.*, **103**, No. 3: 357 (2001).
7. M. Dutkiewicz, A. Velychkovych, I. Shatskyi, and V. Shopa, *Mater.*, **15**, No. 13: 4671 (2022).
8. I. Shatskyi, I. Vytvytskyi, M. Senyushkovych, and A. Velychkovych, *IOP Conf. Ser.: Mater. Sci. Eng.*, **564**: 12073 (2019).
9. A. Velychkovych, *Eng. Solid Mechanics*, **10**, No. 3: 287 (2022).
10. S. Noga, E. Rejman, P. Bałon, B. Kiełbasa, R. Smusz, and J. Szostak, *Acta Mechanica et Automatica*, **16**, No. 3: 215 (2022).
11. S. Dobrotvorskiy, M. Balog, Y. Basova, L. Dobrovolska, and A. Zinchenko, *Advanced Manufacturing Processes* (Eds. V. Tonkonogyi, V. Ivanov, J. Trojanowska, G. Oborskyi, M. Edl, I. Kuric, I. Pavlenko, and P. Dasic) (Cham: Springer: 2020), p. 32.
12. L. S. Saakiyan, A. P. Efremov, and L. Ya. Ropyak, *Zashchita Metallov*, **25**, No. 2: 185 (1989) (in Russian).
13. T. Shihab, P. Prysyazhnyuk, R. Andrusyshyn, L. Lutsak, O. Ivanov, and I. Tsap, *Eastern-European J. Enterprise Technol.*, **1**, No. 12 (103): 38 (2020).
14. T. M. Radchenko, O. S. Gatsenko, V. V. Lizunov, and V. A. Tatarenko, *Prog. Phys. Met.*, **21**, No. 4: 580 (2020).
15. A. B. Melnick, V. K. Soolshenko, and K. H. Levchuk, *Metallofiz. Noveishie Tekhnol.*, **42**, No. 10: 1387 (2020).
16. Ya. Kusyi, V. Stupnytskyy, O. Onysko, E. Dragašius, S. Baskutis, and R. Chatys, *Eksploatacja i Niezawodnosc—Maintenance and Reliability*, **24**, No. 4: 655 (2022).
17. Y. M. Kusyi and A. M. Kuk, *J. Phys.: Conf. Ser.*, **1426**: 012034 (2020).
18. W. Dai, C. Li, D. He, D. Jia, Y. Zhang, and Z. Tan, *Surf. Coat. Technol.*, **380**: 125014 (2019).
19. V. B. Kopei, O. R. Onysko, and V. G. Panchuk, *J. Phys.: Conf. Ser.*, **1426**, No. 1: 012033 (2020).
20. I. Drach, V. Royzman, A. Bubulis, and K. Juzėnas, *Mechanika*, **27**, No. 1: 45 (2021).
21. V. Kotsyubynsky, L. Shyyko, T. Shihab, P. Prysyazhnyuk, V. Aulin, and V. Boichuk, *Mater. Today: Proc.*, **35**, No. 4: 538 (2019).
22. M. Bembenek, J. Krawczyk, and K. Pańcikiewicz, *Eng. Failure Analysis*, **142**: 106843 (2022).
23. N. Senin and L. Blunt, *Characterisation of Areal Surface Texture* (Ed. R. Leach) (Berlin, Heidelberg: Springer: 2013), p. 179.
24. V. S. Protsenko, L. S. Bobrova, S. A. Korniy, A. A. Kityk, and F. I. Danilov, *Funct. Mater.*, **25**, No. 3: 539 (2018).
25. V. S. Protsenko, L. S. Bobrova, A. S. Baskevich, S. A. Korniy, and F. I. Danilov, *J. Chem. Technol. Metallurgy*, **53**, No. 5: 906 (2018).
26. L. Ropyak and V. Ostapovych, *Eastern-European J. Enterprise Technol.*, **2**, No. 5: 50 (2016) (in Ukrainian).
27. O. Bazaluk, O. Dubei, L. Ropyak, M. Shovkoplias, T. Pryhorovska, and V. Lozynskyi, *Energies*, **15**, No. 1: 83 (2022).
28. O. Ya. Dubei, T. F. Tutko, L. Ya. Ropyak, and M. V. Shovkoplias, *Metallofiz. Noveishie Tekhnol.*, **44**, No. 2: 251 (2022) (in Ukrainian).
29. V. I. Lavrinenko, A. G. Lubnin, V. M. Tkach, I. P. Fesenko, and V. V. Smokvyna, *J. Superhard Materials*, **43**, No. 2: 145 (2021).

30. S. I. Kryshtopa, D. Y. Petryna, I. M. Bogatchuk, I. B. Prun'ko, and V. M. Mel'nyk, *Mater. Sci.*, **53**, No. 3: 351 (2017).
31. V. B. Tarelnik, O. P. Gaponova, E. V. Konoplyantschenko, N. S. Yevtushenko, and V. A. Gerasimenko, *Metallofiz. Noveishie Tekhnol.*, **11**, No. 6: 795 (2018).
32. V. M. Holubets, M. I. Pashechko, K. Dzedzic, J. Borc, and A. V. Tisov, *J. Friction Wear*, **41**, No. 5: 443 (2020).
33. V. V. Shyrokov, K. B. Vasyliv, Z. A. Duryahina, H. V. Laz'ko, and N. B. Rats'ka, *Mater. Sci.*, **45**, No. 4: 473 (2009).
34. S. A. Klimenko, I. A. Podchernjaeva, V. M. Beresnev, V. M. Panashenko, S. An. Klimenko, and M. Yu. Kopeikina, *J. Superhard Materials*, **36**, No. 3: 208 (2014).
35. L. Ropyak, T. Shihab, A. Velychkovych, V. Bilinskyi, V. Malinin, and M. Romaniv, *Ceramics*, **6**, No. 1: 146 (2023).
36. M. M. Student, I. B. Ivasenko, V. M. Posuvailo, H. H. Veselivs'ka, A. Y. Pokhmurs'kyi, Y. Y. Sirak, and V. M. Yus'kiv, *Mater. Sci.*, **54**, No. 6: 899 (2019).
37. L. Y. Ropyak, A. S. Velychkovych, V. S. Vytvytskyi, and M. V. Shovkoplias, *J. Phys.: Conf. Ser.*, **1741**, No. 1: 012039 (2021).
38. M. Bembenek, P. Prysyazhnyuk, T. Shihab, R. Machnik, O. Ivanov, and L. Ropyak, *Mater.*, **15**, No. 14: 5074 (2022).
39. B. O. Trembach, M. G. Sukov, V. A. Vynar, I. O. Trembach, V. V. Subbotina, O. Yu. Rebrov, O. M. Rebrova, and V. I. Zakiev, *Metallofiz. Noveishie Tekhnol.*, **44**, No. 4: 493 (2022).
40. J. Pawlik, J. Cieślik, M. Bembenek, T. Gyral, S. Kapayeva, and M. Kapkenova, *Mater.*, **15**, No. 17: 6019 (2022).
41. T. A. Shihab, L. S. Shlapak, N. S. Namer, P. M. Prysyazhnyuk, O. O. Ivanov, and M. J. Burda, *J. Phys.: Conf. Ser.*, **1741**: 012031 (2021).
42. S. P. Chenakin, B. N. Mordyuk, and N. I. Khripta, *Appl. Surf. Sci.*, **470**: 44 (2019).
43. D. Pavlenko, E. Kondratiuk, Y. Torba, Y. Vyshnepolskyi, and D. Stepanov, *Eastern-European J. Enterprise Technol.*, **1**, No. 12 (115): 31 (2022).
44. J. Kusyj and A. Kuk, *Eastern-European J. Enterprise Technol.*, **1**, No. 7 (73): 41 (2015).
45. I. Shepelenko, Y. Tsekhanov, M. Storchak, Y. Nemyrovskyi, and V. Cherkun, *Advanced Manufacturing Processes II* (Eds. V. Tonkonogei, V. Ivanov, J. Trojanowska, G. Oborskyi, A. Grabchenko, I. Pavlenko, M. Edl, I. Kuric, and P. Dasic) (Cham: Springer: 2021), p. 619.
46. O. V. Maksymiv, V. I. Kyryliv, V. P. Chaikovskyi, B. R. Tsizh, A. M. Kostruba, and V. I. Hurei, *Mater. Sci.*, **56**, No. 4: 523 (2021).
47. V. I. Kyryliv, V. I. Gurey, O. V. Maksymiv, I. V. Hurey, and Y. O. Kulyk, *Mater. Sci.*, **57**, No. 3: 422 (2021).
48. A. Raza and S. Kumar, *Tribology International*, **174**: 107717 (2022).
49. W. Brostow, K. Czechowski, W. Polowski, P. Rusek, D. Toboła, and I. Wronska, *Materials Research Innovations*, **17**, No. 4: 269 (2013).
50. D. F. Silva-Álvarez, A. Márquez-Herrera, A. Saldana-Robles, M. Zapata-Torres, R. Mis-Fernández, J. L. Pena-Chapa, J. Moreno-Palmerín, and E. Hernández-Rodríguez, *J. Mater. Research Technol.*, **9**, No. 4: 7592 (2020).
51. M. Bembenek, R. Kudelski, J. Pawlik, and Ł. Kowalski, *Mater.*, **14**, No. 19: 5625 (2021).

52. M. Nalbant, H. Gökkaya, I. Toktaş, and G. Sur, *Robotics and Computer Integrated Manufacturing*, **25**, No. 1: 211 (2009).
53. K. Kumar and K. E. Prasad, *IOSR J. Mechanical and Civil Engineering*, **12** No. 1: 1 (2016).
54. T. G. Mathia, P. Pawlus, and M. Wieczorowski, *Wear*, **271**, No. 3–4: 494 (2011).
55. V. Chomienne, F. Valirgue, J. Rech, and C. Vierdu, *CIRP J. Manufacturing Sci. Technol.*, **13**: 90 (2016).
56. J. T. Maximov, G. V. Duncheva, A. P. Anchev, N. Ganev, I. M. Amudjev, and V. P. Dunchev, *J Braz. Soc. Mech. Sci. Eng.*, **40**: 194 (2018).
57. K. L. Lyon, T. J. Marrow, and S. B. Lyon, *J. Mater. Processing Technol.*, **218**: 32 (2015).
58. W. Koszela, *Head for Performing Lubricating Micropockets on the Surface of the Cylinder Liners*, Patent 217855 PL (Published August, 2014) (in Polish).
59. A. Kochman, *Rotary Fuel Pump Head*, Patent 233483 PL (Published November, 2019) (in Polish).
60. W. Koszela, *Kształtowanie Regularnej Struktury Geometrycznej na Powierzchniach Elementyw Trących* [Formation of a Regular Geometric Structure on the Surfaces of Rubbing Elements] (Rzeszyw: Wydawnictwo Naukowe Instytutu Technologii Eksploatacji w Radomiu: 2015) (in Polish).
61. K. E. Oczoś and V. Liubimov, *Struktura Geometryczna Powierzchni: Podstawy Klasyfikacji z Atlasem Charakterystycznych Powierzchni Kształtowanych* [Geometric Structure of Surfaces, Basics of Classification with an Atlas of Characteristic Shaped Surfaces] (Rzeszyw: Oficyna Wydawnicza Politechniki Rzeszowskiej: 2003) (in Polish).
62. D. Capanidis, *Archives of Civil and Mechanical Engineering*, **7**, No. 4: 39 (2007).
63. C. Gachot, A. Rosenkranz, S. M. Hsu, and H. L. Costa, *Wear*, **372–373**: 21 (2017).
64. T. Dyl, *Archives of Metallurgy and Materials*, **62**, No. 2: 807 (2017).
65. P. Bałon, A. Świątoniowski, E. Rejman, B. Kiełbasa, R. Smusz, J. Szostak, and Ł. Kowalski, *Adv. Sci. Technol. Res. J.*, **14**, No. 2: 155 (2020).
66. *Cogsdill Tool Products. Product Catalogue*, https://www.cogsdill.com/products/burnishing-tools
67. P. Bałon, E. Rejman, B. Kiełbasa, and R. Smusz, *Mechanik*, **95**, No. 11: 43 (2022).
68. M. Korzynski and T. Zarski, *Surf. Coat. Technol.*, **307**, Part A: 590 (2016).
69. J. Kalisz, K. Żak, W. Grzesik, and K. Czechowski, *J. Machine Eng.*, **15**, No. 1: 71 (2015).
70. P. Bednarski, D. Biało, W. Brostow, K. Czechowski, W. Polowski, P. Rusek, and D. Toboła, *Mater. Sci.—Medžiagotyra*, **19**, No. 4: 367 (2013).
71. K. Zaleski, *Technologia Nagniatania Dynamicznego* [Dynamic Burnishing Technology] (Liublin: Wydawnictwo Politechniki Lubelskiej: 2018) (in Polish).
72. *Taylor Hobson. Product Catalogue*, https://www.taylor-hobson.com
73. Z. Wang and D. Gao, *Mater. Des.*, **53**: 881 (2014).
74. A. Codrignani, B. Frohnapfel, F. Magagnato, P. Schreiber, J. Schneider, and P. Gumbsch, *Tribol. Int.*, **122**: 46 (2018).